Identification of individual 4-methylpyridine molecules physisorbed and chemisorbed on $TiO_2(110)$-(1 × 1) surface by STM

Shushi Suzuki, Hiroshi Onishi, Takehiko Sasaki, Ken-ichi Fukui and Yasuhiro Iwasawa *

Department of Chemistry, Graduate School of Science, The University of Tokyo, Hongo, Bunkyo-ku, Tokyo 113-0033, Japan

Received 29 May 1998; accepted 6 August 1998

We succeeded in identifying geometries of 4-methylpyridine (4-MP) molecules adsorbed on a $TiO_2(110)$-(1 × 1) surface based on sequential STM imaging. Characteristics in mobility, topographic height, and location allowed us to distinguish three adsorption states at room temperature: a chemisorbed state with the upright geometry (A_1), a flat-lying state localized at specific sites (A_2), and a flat-lying physisorbed state mobile over the surface (B). The concentration of A_1 and A_2 species was restricted at an order of 0.01 ML. The A_2 state was related to the adsorption at oxygen vacancies resident on the vacuum-annealed surface. The present study demonstrates the promising ability of STM to identify the adsorption geometry of small probe molecules, 4-methylpyridine in the present case, and to provide atom-level information on the origin of acidic property of oxide surfaces.

Keywords: acid–base property, STM, 4-methylpyridine, $TiO_2(110)$, adsorption geometry

1. Introduction

Controlling the acid–base properties of oxide surfaces is the key issue for the development of industrial catalysts [1,2]. The inherent compositional and structural inhomogeneity of metal oxide surfaces, however, makes the problem of identifying the catalytic performance of different sites extremely difficult. For example, pyridine, a typical Lewis-base molecule, has been used as a probe for the acidic property of oxide catalysts [3–9]. By analyzing the adsorbed probe molecules with spectroscopic techniques such as TPD, IR, and NMR, we can determine the strength, quantity, and character (Lewis type or Brønsted type) of acid sites on an examined catalyst. It is still difficult to identify where the molecules of a particular state determined by the macroscopic spectroscopy are adsorbed on the surface of inhomogeneity.

Scanning tunneling microscopy (STM) has a great potential to overcome the problem of heterogeneity, since individual events at each surface site should be discriminated by this method. In fact, we have succeeded in visualizing individual pyridine molecules adsorbed on a rutile $TiO_2(110)$-(1 × 1) surface at 300 K [10,11]. Figure 1 shows a bulk-terminated model of the $TiO_2(110)$ surface with a single atom height step parallel to the [1$\bar{1}$2] direction. Surface-exposed titanium atoms on the perfect (110) terrace are five-fold coordinated with oxygen atoms, whereas Ti atoms at the step edge are four-fold coordinated. A pyridine admolecule on the terrace was weakly physisorbed on the five-fold coordinated site and hence very mobile at 300 K so that the topography of the molecules could not be recorded in the time scale of scanning (∼1 s) [11]. In contrast, molecules adsorbed on the four-fold coordinated sites exposed on the step edge of the particular orientation, which may perhaps be chemisorbed, exhibited a topography immobile at the adsorption sites over 100 s [10]. Real-time STM imaging is thus a powerful tool to observe the mobility difference of adsorbed probe molecules. However, the adsorption geometry of pyridine (figure 2) could not be identified by the STM observations, probably because the topographic height difference between upright and flat-lying geometries is small for this compound. In the present study, we em-

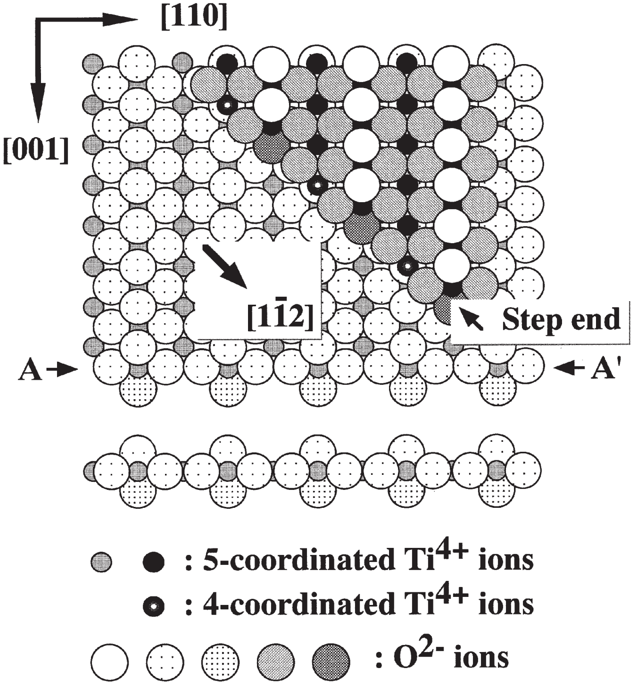

Figure 1. A model of $TiO_2(110)$-(1 × 1) surface with a single height step along the direction. A top view and A–A′ cross section are shown.

---

[*] To whom correspondence should be addressed.

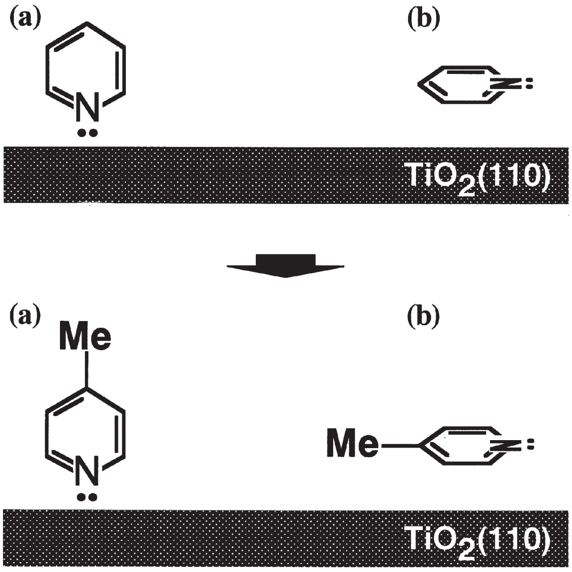

Figure 2. Schematic drawings of pyridine and 4-methylpyridine probe molecules in (a) a flat-lying physisorbed state, and (b) an upright chemisorbed state.

ployed 4-methylpyridine (4-MP) instead of pyridine as a probe. One methyl group substituted at the *para*-position of the six-membered ring should enhance the topographic difference between the two states. The present Letter briefly reports that three states of 4-MP adsorbed on the (110) terrace with oxygen vacancies were identified by combining the mobility analysis and height analysis of sequential STM images. The full results including the adsorption at the step sites will be presented elsewhere [12].

2. Experimental

The experiments were performed with an UHV compatible scanning tunneling microscope (JSTM-4500VT, JEOL) equipped with an Ar^+ gun and LEED-AES optics. A polished rutile TiO_2(110) wafer of $6.5 \times 1 \times 0.25$ mm^3 (Earth Chemicals) was annealed in air at 1100 K for 1 h. A nickel film was deposited in a separate chamber on the back side of the wafer for resistive heating on the microscope stage. The temperature of the surface was monitored with an IR radiation thermometer. After cycles of Ar^+ sputtering (3 keV, 0.3 μA) and vacuum-annealing at 900 K, the surface showed a sharp (1×1) LEED pattern. The (1×1) surface cooled to room temperature was exposed to 4-methylpyridine (research grade, Wako Pure Chemicals) vapor in the treatment chamber and then transferred on the microscope stage without breaking vacuum. Constant current topography of the 4-MP-exposed surface was continuously observed at room temperature in UHV ($\sim 2 \times 10^{-8}$ Pa) with an electro-chemically etched W tip and recorded in video. A positive sample bias voltage (V_s) of +2.0 V and a tunneling current (I_t) of 0.05 nA were employed in imaging.

3. Results and discussion

The annealed TiO_2(110)-(1×1) surface was exposed to 0.03 L of 4-methylpyridine (4-MP) vapor at room temperature and then transferred on the microscope stage. Figure 3 (a)–(c) shows STM images sequentially recorded on the 4-MP-exposed surface. Adparticles of completely circular shape and incomplete, fragmented shapes were observed on the terrace. Those features were assigned to adsorbed 4-MP molecules, since they were not observed before the exposure. Three classes of molecules could be identified based on their mobility, topographic height, and location.

By animating a number of sequential images, the mobility of admolecules could be easily differentiated. Molecules labeled A_1 in figure 3(a), the least mobile state, stayed over 15 min at their original positions during the course of imaging, a part of which is presented in figure 3. Those immobile 4-MP molecules exhibited a complete circular topography, since they were fixed in the time scale of tip scanning. A less stable state A_2 also seemed immobile at first sight. In image (a) there are four A_2 molecules. Three of these (except for the bottom left one) were half imaged in at least one of the sequential images recorded within 40 s, showing their diffusion on the surface. However, admolecules were again imaged at the same positions in the subsequent images. This indicates that A_2-state 4-MP molecules were trapped and liberated repeatedly at specific sites. The last class, B state, contained molecules of nearly circular topographies labeled and of unlabeled fragmented images, as shown in figure 3. They were quite mobile and easily differentiated from A_1 and A_2 species by animating sequential images. If we assume that a fragmented image corresponds to one 4-MP molecule, the concentration of B species was much larger than the population of the two other states.

The difference in topographic height supported the identification of A_1, A_2, and B states. Figure 4 summarizes the results of cross section curves of molecules in the three states. The topography of pyridine adsorbed on this surface is also presented [11]. The A_1 state gave rise to the largest protrusion of 0.34 ± 0.02 nm (averaged on 10 molecules), while the height of the A_2 state was 0.26 ± 0.02 nm (averaged on 11 molecules). A_1- and A_2-state molecules could be safely distinguished on the topographic heights. Corrugation of species B, 0.25 ± 0.02 nm (averaged on 29 molecules), was compatible with the corrugation of the A_2 state. The in-plain width of A_2 species was larger than those of A_1 and B states.

The adsorbed position relative to the Ti-row was also different for A_1 and A_2. A_1-state molecules were always adsorbed just on the Ti-rows, whereas the image center of species A_2 was shifted away from the Ti-row, as illustrated in figure 3(b) where the position of the Ti-rows was marked with white lines for clarity. The location of B species was sometimes difficult to be determined precisely, because they gave often only a fragmented image due to quick migration.

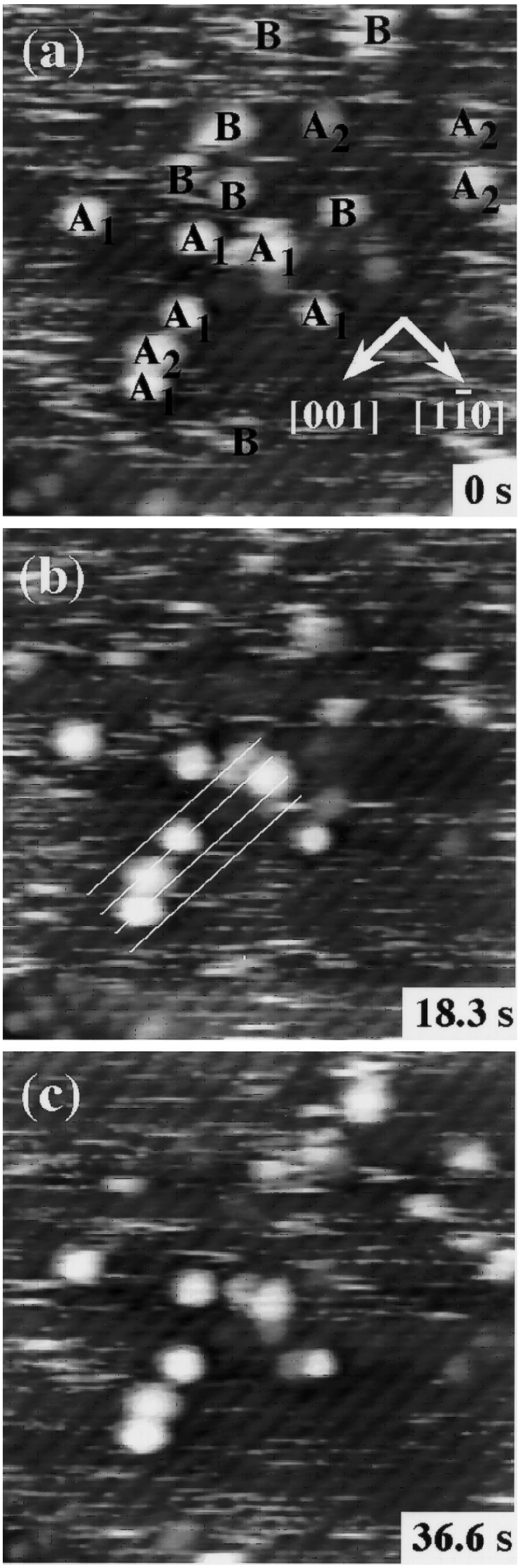

Figure 3. Sequential STM images of the 4-methylpyridine-exposed $TiO_2(110)$-(1 × 1) surface. 15 × 15 nm^2, sample bias voltage: +2.0 V, tunneling current: 0.05 nA.

When a B-state molecule stayed long enough for proper imaging, its topography was centered on a Ti-row.

Three different adsorption states of 4-MP were thereby distinguished with the characteristics in mobility, topographic height, and location. Here we consider the identity of those states. The most mobile state B is assigned to a physisorbed state. Molecular topography of similar mobility and height was observed on the pyridine-exposed $TiO_2(110)$ surface and assigned to pyridine molecules physisorbed in flat-lying geometry, on the basis of thermal desorption, XPS and molecular dynamics calculation results [11].

The less mobile A_1 and A_2 species should be bound to the surface more strongly with higher barrier against migration. If we assume that the image height determined in figure 4 reproduces the physical topography of the imaged molecule, the height difference of 0.08 nm can be attributed to the difference in adsorption geometry, upright or flat-lying. The height of A_2 species compatible with the corrugation of B state suggests a flat-lying geometry of A_2-state molecules. The A_1 state of largest corrugation is assigned to the 4-MP molecule adsorbed with the aromatic ring vertical to the surface. Figure 5 illustrates the proposed geometries. One would expect that the height difference between molecules with the aromatic ring parallel and vertical to the surface would be greater than 0.08 nm. For instance, the van der Waals height of toluene is estimated to be 0.8 nm, while its thickness is 0.4 nm. Our simple assumption is supported by a systematic observation of the image height of formate, acetate, and pivarate (trimethylacetate) ions adsorbed on the $TiO_2(110)$ surface. The image height of the carboxylate ions were 0.15, 0.25, and 0.45 nm, respectively [12]. Because those carboxylates should be adsorbed in bridge form, the increase in image height is related with the size of the alkyl group. By substituting a hydrogen atom with a methyl group, image height increased by 0.10 nm from formate to acetate, and by 0.20 nm from acetate to pivalate. One methyl group, the

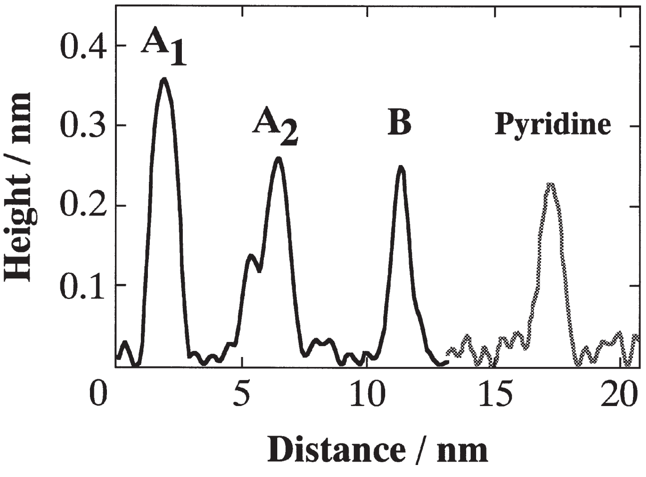

Figure 4. Cross sections of STM topography of different states of the 4-methylpyridine molecule, and the flat-lying physisorbed state of the pyridine molecule on the $TiO_2(110)$-(1 × 1) surface.

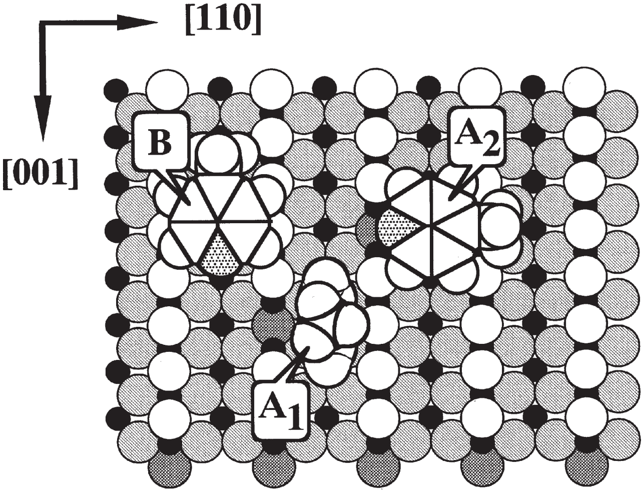

Figure 5. A pictorial model of A_1, A_2, and B states of 4-methylpyridine molecules adsorbed on the $TiO_2(110)$-(1 × 1) surface.

van der Waals radius of which is 0.2 nm, induced a much smaller increase in image height. This is well known as an artifact of "tunnel vision" resulting from the dominant contribution of electronic effects in tunneling.

The upright geometry A_1 naturally leads to a chemisorbed state with a definite N–Ti bond. The concentration of this state was not more than 0.01 ML. The restricted population is reasoned if we assume that the formation of this chemisorbed state is an activated process with a small sticking coefficient at room temperature.

A flat-lying geometry of the A_2 state was suggested by the height analysis. On the other hand, A_2 species were much less mobile than the B-state physisorbed molecules. As mentioned above, detailed inspection of the sequential STM images revealed that the A_2-state molecules trapped and liberated repeatedly at specific sites. These experimental results can be interpreted by assuming that A_2 species are adsorbed at oxygen vacancies in a flat-lying geometry. Actually, an empirical molecular dynamics calculation predicted a flat-lying state of pyridine is more strongly bound at a point vacancy of bridge oxygen than on the perfect terrace by 8 kJ/mol [12]. Oxygen vacancies are easily created on vacuum-annealed $TiO_2(110)$ surfaces [13], and recently visualized by atomic force microscopy operated in a frequency-modulated non-contact mode (NC-AFM) [14]. The number density of the vacancies observed with NC-AFM was 0.02 ML, which is comparable to the coverage of A_1-state molecules obtained in the present study.

The mobile physisorbed state was majority species of 4-MP and pyridine on the $TiO_2(110)$-(1 × 1) surface. This verifies that the five-fold coordinated Ti^{4+} ion exposed to the surface is incapable of forming stable N–Ti bonds with the basic nitrogen atoms of those compounds, being in accordance with the weak acidic character observed on rutile TiO_2 catalysts [15]. Weak Lewis-acidic property of the Ti centers, and the electrostatic repulsion between the protruding bridge oxygen atoms and the aromatic ring of the probe molecules likely causes the unexpected absence of activity.

In summary, three different states of 4-methylpyridine adsorbed on the $TiO_2(110)$-(1 × 1) surface were distinguished with the characteristics in mobility, topographic height, and location, which were determined by analysis of sequential STM topographies: a chemisorbed state with the upright geometry (A_1), a flat-lying state localized at specific sites (A_2), and a flat-lying physisorbed state mobile over the surface (B). The concentration of A_1 and A_2 species was restricted at an order of 0.01 ML. The A_2 state was related to the adsorption at oxygen vacancies resident on the vacuum annealed surface. The present study demonstrates the promising ability of STM to identify the adsorption geometry of small probe molecules, 4-methylpyridine in the present case, and to provide atom-level information on the origin of acidic property of oxide surfaces.

Acknowledgement

This work has been supported by Core Research for Evolutional Science and Technology (CREST) of the Japan Science and Technology Corporation (JST).

References

[1] Y. Iwasawa, in: *Proc. 11th Int. Congr. Catalysis*, Stud. Surf. Sci. Catal., Vol. 101, eds. J.W. Hightower, W.N. Delgass, E. Iglesia and A.T. Bell (Elsevier, Amsterdam, 1996) p. 21.
[2] Y. Iwasawa, Catal. Surveys Jpn. 1 (1997) 3.
[3] A.M. Youssef, M.N. Alaya and M.A. Hamada, Thermochim. Acta 235 (1994) 91.
[4] I.E. Wachs, Catal. Today 27 (1996) 437.
[5] C. Morterra, G. Ghiotti and E. Garrone, J. Chem. Soc. Faraday Trans. I 76 (1980) 2102.
[6] M. Waqif, J. Bachelier, O. Saur and J.C. Lavalley, J. Mol. Catal. 72 (1992) 127.
[7] M. Delarco, S.R.G. Carrazan, C. Martin and V. Rives, J. Mater. Sci. 31 (1996) 1561.
[8] T. Kataoka and J.A. Dumesic, J. Catal. 112 (1988) 66.
[9] A. Hess and E. Kemnitz, Appl. Catal. A 149 (1997) 373.
[10] S. Suzuki, Y. Yamaguchi, H. Onishi, K. Fukui, T. Sasaki and Y. Iwasawa, Catal. Lett. 50 (1998) 117.
[11] S. Suzuki, Y. Yamaguchi, H. Onishi, T. Sasaki, K. Fukui and Y. Iwasawa, J. Chem. Soc. Faraday Trans. 94 (1998) 161.
[12] S. Suzuki, H. Onishi, T. Sasaki, K. Fukui and Y. Iwasawa, to be submitted.
[13] V.E. Henrich and P.A. Cox, *The Surface Science of Metal Oxides* (Cambridge University Press, Cambridge, 1994).
[14] K. Fukui, H. Onishi and Y. Iwasawa, Phys. Rev. Lett. 79 (1997) 4202.
[15] M. Ueshima, K. Sano, M. Ikeda, K. Yoshino and J. Okamura, Res. Chem. Intermed. 24 (1998) 133.